

## Radiative lifetimes in Si I from laser-induced fluorescence in the visible, ultraviolet, and vacuum ultraviolet

T. R. O'Brian\* and J. E. Lawler

*Department of Physics, University of Wisconsin, Madison, Wisconsin 53706*

(Received 26 August 1991)

Radiative lifetimes for 47 levels in neutral silicon are reported. Lifetimes are measured using time-resolved laser-induced fluorescence (LIF) on a beam of silicon atoms. The transitions studied span the spectral range 160–410 nm. The experimental methods used are broadly applicable for measuring lifetimes in almost any neutral or singly ionized element using LIF in the visible, ultraviolet, and vacuum-ultraviolet spectral regions. Lifetimes are combined with previously reported branching fractions or branching ratios to generate 36 absolute transition probabilities, most with total uncertainty of 5–10%.

PACS number(s): 32.70.Fw, 97.10.Tk

### INTRODUCTION

Silicon contributes substantially to ultraviolet solar and stellar opacity through its high abundance [ $\log_{10}(N_{\text{Si}}/N_{\text{H}}) = -4.45$  in the sun [1]], and rich ultraviolet spectrum. The study of astrophysical elemental abundance and synthesis of stellar spectra for nearly all elements, including silicon, is limited by the accuracy of existing atomic transition probabilities [2,3]. Accurate relative transition probabilities for silicon are available from careful emission and absorption experiments [4,5]. Much less certain is the correct normalization to convert relative transition probabilities to the absolute transition probabilities necessary for abundance determinations and synthesis of stellar spectra containing silicon lines. Smith *et al.*, reporting extensive measurements of relative transition probabilities, discussed the need for additional lifetime measurements in neutral silicon [5]. It is widely thought that the combination of accurate atomic-level radiative lifetimes with precisely measured branching fractions provides the best experimental determination of absolute transition probabilities [6,7]. Measurement of as many upper-level lifetimes as possible, covering as broad a range of upper-level energies as possible, permits the most accurate determination of absolute transition probabilities. Reported in this paper are the lifetimes of 47 upper levels in neutral silicon ranging in energy from 39 000 to 63 000  $\text{cm}^{-1}$ , measured by time-resolved laser-induced fluorescence on a slow atomic beam of silicon using radiative transitions in the visible, ultraviolet, and vacuum-ultraviolet (vuv) regions between 160 and 410 nm. The lifetimes reported in this paper are of particular interest because they involve extensive measurements of levels with transitions primarily or exclusively in the vacuum ultraviolet (<200 nm), span a broad range of upper-level energies (39 000–63 000  $\text{cm}^{-1}$ ), and represent a major increase in the number and precision of measured lifetimes in silicon. These three issues are addressed in the paragraphs below.

Spectrographs on orbiting observatories such as the International Ultraviolet Explorer and the Goddard High

Resolution Spectrograph on the Hubble Space Telescope have already generated a substantial data base of vuv spectra requiring accurate atomic transition probabilities for interpretation. Some species, such as neutral silicon, have most of their transitions in the vuv or far infrared, inaccessible to ground-based observation. Many of the important resonance transitions for neutral and ionized species lie in the vuv. Such resonance transitions are particularly vital to studies of the interstellar medium where absorption of radiation is primarily from ground or near-ground levels of atoms and ions in the relatively cold medium. The method of measuring lifetimes for vuv transitions presented in this paper is broadly applicable to neutral and singly ionized atoms of almost any element.

The wide range of upper-level energies studied in this experiment (extending nearly to the ionization limit at 65 700  $\text{cm}^{-1}$ ), when applied to silicon emission spectra from sources operated near Boltzmann equilibrium, means it will be possible to measure the absolute transition probabilities to 5–10% accuracy for essentially all of the classified transitions in neutral silicon using methods pioneered by Whaling and co-workers [8,9]. Combining lifetimes with branching fractions will directly result in accurate absolute transition probabilities for numerous transitions. Using these transition probabilities, the relative populations of the upper levels in an emission source can be determined. If the level populations approximate a Boltzmann distribution (that is, if local thermodynamic equilibrium is nearly achieved), then the relative populations of levels energetically close to the reference levels can be interpolated on a Boltzmann plot of relative population as a function of level energy. The relative populations can then be used to calculate the transition probabilities relative to the reference levels. When the reference levels (both lifetimes and branching fractions directly measured) are distributed over a broad energy range, populations of nearby levels can be accurately interpolated, even when the source departs somewhat from local thermodynamic equilibrium (LTE). The difficulties in truly achieving LTE in an emission source

are well known and represent a major challenge to the accurate measurement of transition probabilities through emission experiments alone. However, even when LTE is not attained, a high-pressure source can closely approximate Boltzmann equilibrium over small energy spans due to collisional mixing between energy levels closely spaced compared to the average translational energy of the atoms and ions (e.g., a few thousand  $\text{cm}^{-1}$  for sources with effective temperatures of about 5000 K). When the reference levels are spaced more closely than  $k_B T$ , interpolation between the reference levels results in accurate relative populations (and thus transition probabilities) despite the absence of complete LTE. Since the silicon lifetimes measured in this paper span a broad range of upper-level energies and those energies are closely spaced, accurate determination of absolute transition probabilities for essentially all classified transitions in silicon should be possible when the lifetime data are applied to the emission spectrum of a silicon source operating near LTE.

Only a few measured lifetimes in silicon have been previously reported, and most of those were determined by time-of-flight beam-foil spectroscopy [10] or by electron-excitation phase-shift techniques [11,12]. While beam-foil spectroscopy currently represents the best practical method for determining lifetimes of highly ionized species, it is less satisfactory for neutral or singly ionized species [13]. Both beam-foil and phase-shift techniques use nonselective excitation of upper levels with resultant cascade repopulation of the studied level from simultaneously excited higher-lying levels. This cascade repopulation distorts the natural (single exponential) decay of the target level. Selective excitation of upper levels in LIF experiments such as the one reported here eliminates the cascade repopulation problem, and the signals obtained are generally quite strong. The use of pulsed tunable laser excitation and time resolution of the resultant fluorescence signal routinely results in level lifetimes independently reproducible to 5% accuracy [6]. Under favorable conditions, it is possible to measure lifetimes to a precision of 1% or better using LIF techniques [14], and certain studies require such precision [3]. However, most astrophysical applications are better served by extensive sets of transition probabilities to 5–10% accuracy than by a few isolated measurements of higher precision.

The methods described in this paper represent an important extension into the vuv of the experiments developed by Duquette, Salih, and Lawler to measure the radiative lifetimes of essentially any neutral or singly ionized atomic species [15,16]. A low-pressure, large-bore hollow cathode discharge (HCD) source is used to produce slow atomic and ionic beams. The source has been used to measure lifetimes by LIF on neutral and singly ionized atoms for more than 30 elements so far. Pulsed, continuously tunable laser radiation in the visible, ultraviolet, and vacuum ultraviolet is generated by a Nd:YAG (where YAG denotes yttrium aluminum garnet) laser-pumped or nitrogen laser-pumped dye laser, with second-harmonic generation in crystals and stimulated Raman scattering in hydrogen gas when necessary. The

experiment provides complete spectral coverage of the region 150–700 nm, and minor modifications will extend the lower wavelength limit to near 100 nm. The 100–200-nm spectral region is particularly important in vuv astronomy because of the large number of resonance transitions and the transparency of interstellar hydrogen (apart from the Lyman lines) in this region.

## EXPERIMENTAL METHODS

Two different experimental systems were used in this study as depicted schematically in Figs. 1 and 2. One system provides spectral coverage in the visible and ultraviolet (about 210–700 nm) and the second provides spectral coverage into the vacuum ultraviolet (about 150–700 nm). The HCD beam sources used in each experiment are essentially identical. In each system, the HCD source generates an uncollimated beam of slow silicon atoms. Pulsed laser radiation, orthogonal to the atomic beam, is tuned to selectively excite a single atomic upper level. Laser-induced fluorescence from the decay of the excited upper level is detected orthogonally to both the laser and atomic beams by an  $f/1$  imaging system and a photomultiplier tube. The fluorescence signal from the photomultiplier tube is processed by a fast transient digitizer. Several hundred decays are averaged and automatically analyzed to generate a radiative lifetime. Reported lifetimes represent the average of several thousand decays.

The low-pressure, large-bore HCD beam source

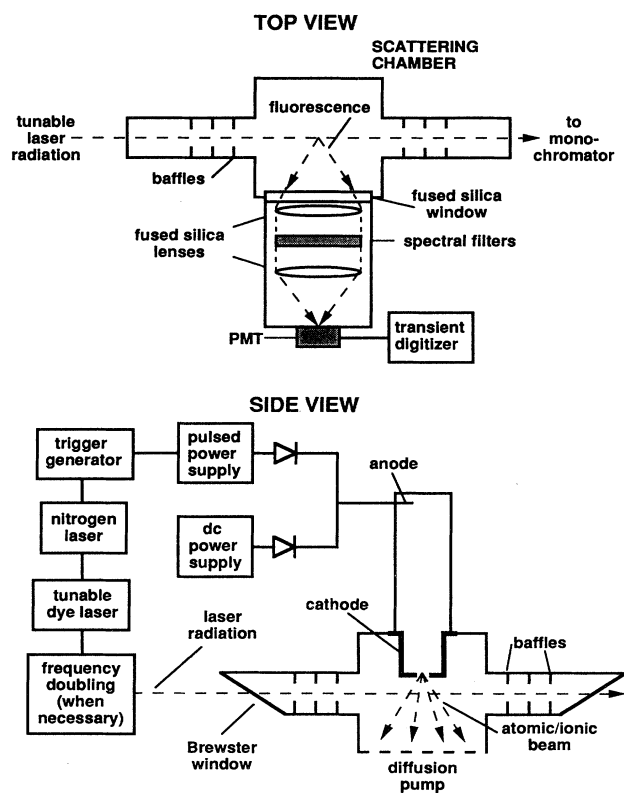


FIG. 1. Schematic diagram of the visible-ultraviolet lifetime experiment (spectral range 210–700 nm).

cathode is a stainless-steel tube (29-mm inner diameter, 50 mm long), sealed at one end except for a 1.0-mm-diam opening flared outward to form an uncollimated atomic beam or ionic beam. The cathode is lined with the element to be studied, which is sputtered by a dc discharge of about 50 mA in continuously flowing argon gas at a pressure of about 0.5 Torr. Three different types of sil-

icon liners were used successfully: strips of high-purity (99.9999%) silicon cleaved from silicon wafers and arranged "barrel-fashion" around the inside of the steel cathode; thin (0.025–0.050 mm) sheets of metallic glass foils containing about 10% silicon (as well as iron or cobalt and boron); and a high-purity (99.9999%) thin-walled (0.5 mm) tube of silicon custom fabricated to fit the steel cathode. All three sources generated a useful flux of silicon atoms, although the pure silicon cylinder proved the most effective sputter source. The metallic glass foils produce a good flux of silicon atoms, but the other constituents are also sputtered, potentially producing blends with silicon transitions. Sputtered atoms along with the argon carrier gas emerge from the cathode nozzle into a scattering chamber held at much lower pressure (about  $10^{-4}$  Torr) by a diffusion pump. A pulsed power supply permits superposition of 5–10  $\mu$ s current pulses of up to 12 A on the dc discharge current. Such pulses produce an intense burst of silicon atoms and ions distributed among many metastable levels, permitting study of weak transitions and of transitions not directly connected to the ground level. In silicon, useful populations in even parity levels up to  $3p^2^1S_0$  (15 394  $\text{cm}^{-1}$  above the ground level) are found, increasing the number of accessible odd parity upper levels. A detailed description of the HCD source including dimensions and materials has been previously published [17].

In both systems (visible-ultraviolet and vacuum ultraviolet) the laser beam crosses the atomic beam 1 cm below the nozzle. Continuous spectral coverage from 210 to 700 nm is provided by a nitrogen laser-pumped dye laser with second-harmonic generation (when necessary) in potassium dihydrogen phosphate (KDP) or  $\beta$ -barium borate crystals. The nitrogen laser-pumped dye laser produces 3-ns pulses [full width at half maximum (FWHM)] with a bandwidth of  $0.2 \text{ cm}^{-1}$  and peak power up to 40 kW. Continuous spectral coverage from 150 to 700 nm is provided by a Nd:YAG laser-pumped dye laser with second-harmonic generation in KDP and stimulated Raman scattering (SRS) in hydrogen gas when necessary. Although both laser systems provide coverage of the visible and ultraviolet regions, in practice the nitrogen laser-pumped system is generally preferred for excitation transitions above 210 nm due to greater ease and lower cost of operation.

Deep-ultraviolet and vacuum-ultraviolet laser radiation is generated by anti-Stokes SRS, in liquid nitrogen-cooled hydrogen gas, of the second harmonic of a pulsed, Nd:YAG-pumped dye laser. Nonresonant SRS provides the continuous tunability in the vacuum ultraviolet (in this case  $\geq 160 \text{ nm}$ ) necessary for a comprehensive survey of level lifetimes. Competitive vuv laser techniques, such as sum and difference frequency mixing in metal vapors or noble gases, can be significantly more efficient in generating vuv radiation, but for most of the vuv tunability is limited to narrow spectral regions around atomic resonances in the conversion medium, and continual adjustments in the buffer gas are necessary to ensure phase matching at different wavelengths.

The Nd:YAG pump laser produces 10-ns-long (FWHM), 200-mJ pulses in the second harmonic (532

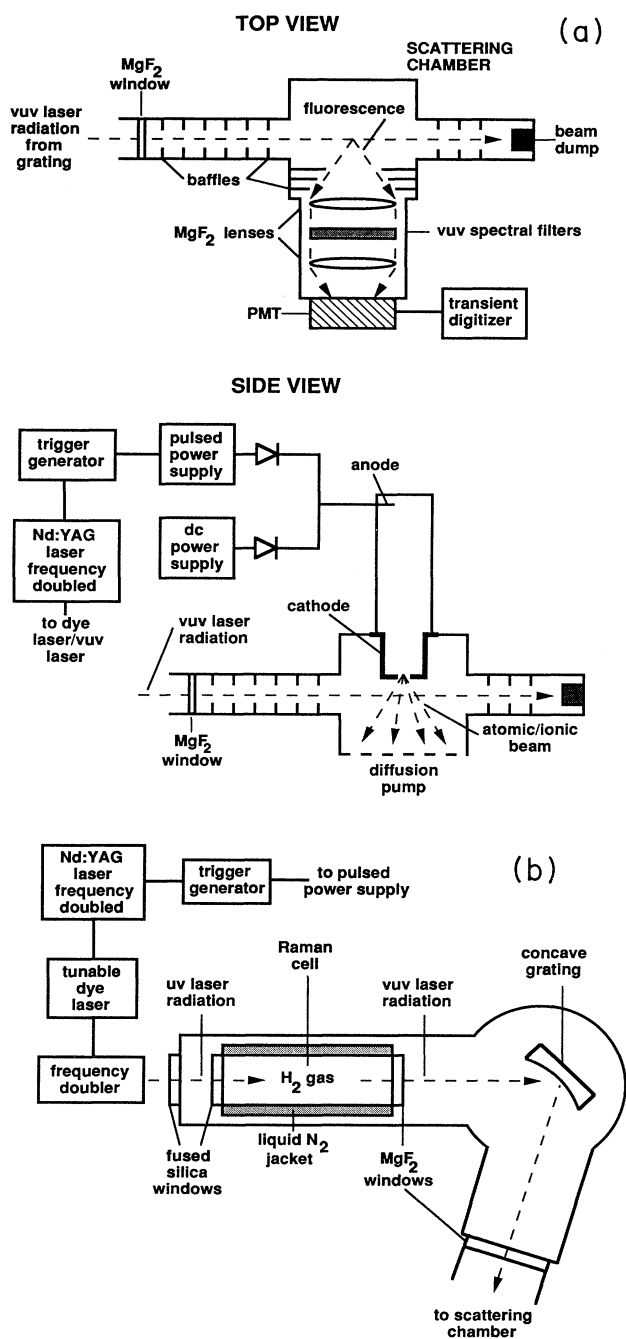


FIG. 2. Schematic diagram of the vacuum-ultraviolet lifetime experiment (current spectral range 150–700 nm). (a) Beam source and scattering chamber. (b) Vacuum-ultraviolet laser system.

nm) with a 27-Hz repetition rate. Dye-laser pulses with energies up to 50 mJ in the range 540–640 nm, collimated to a 5-mm-diam beam, are frequency doubled in KDP (270–320 nm). The approximately 8-mJ second-harmonic pulses, along with the unconverted dye-laser fundamental radiation, are focused with a 25-cm focal-length lens into the center of the Raman cell. The cell is a 30-cm-long, 2.5-cm-inner-diameter stainless-steel tube filled with about  $2.5 \times 10^5$  Pa (at 77 K) of hydrogen gas. The fused silica input window and magnesium fluoride output window of the Raman cell are sealed to the tube with indium metal gaskets, permitting repeated cycling between room temperature and 77 K [18]. A mixture of several orders of Stokes shifted, anti-Stokes shifted, and unconverted dye-laser radiation diverges out of the Raman cell. Each anti-Stokes order is blueshifted by  $4155 \text{ cm}^{-1}$  from the preceding order. A concave holographic diffraction grating (1200 lines/mm, 5 cm diameter, 1 m radius of curvature) disperses the various anti-Stokes orders (and other radiation) and images the desired order into a 5-mm circular beam 1 cm below the atomic beam nozzle. The concave grating, in a modified Seya-Namioka mount [19], produces an astigmatic image of the off-axis incident laser radiation—the circle of least confusion falls near the atomic beam. The regions around the Raman cell, the grating, and the laser beam path up to the scattering chamber are maintained in an oil-free vacuum of about  $10^{-7}$  Torr by an ion pump. The scattering chamber is held under separate vacuum (about  $10^{-4}$  Torr of argon when the beam source is operating) by a diffusion pump, and a magnesium fluoride window separates the two vacuum systems.

Each nonlinear step in the generation of the vuv radiation temporally compresses the laser pulse. The higher-order anti-Stokes pulses used in this study (up to the seventh anti-Stokes order) have a duration of 4–5 ns (FWHM). The dye-laser bandwidth of about  $0.3 \text{ cm}^{-1}$  is slightly broadened in the SRS process, probably by the ac Stark effect [20]. The anti-Stokes Raman orders have an estimated bandwidth of  $0.5 \text{ cm}^{-1}$ . For the silicon transitions studied, this small bandwidth degradation posed no problems—all transitions were easily resolved. The vuv laser system as currently configured generates useful amounts of radiation of wavelengths as short as 150 nm (eighth anti-Stokes order). Modest improvements in the pump laser power should extend the useful wavelength range to below 130 nm [21]. Below about 130 nm, sum frequency mixing in mercury vapor proceeding through autoionizing levels and providing nearly continuous tunability may be superior to SRS [22–24].

In both the visible-ultraviolet (vis-uv) and vuv systems, the LIF from the atomic beam is detected orthogonally to both the laser and atomic beams by an  $f/1$  fluorescence collection system and a fast photomultiplier tube. The vis-uv system uses two fused silica lenses and an RCA 1P28A photomultiplier tube, all at atmospheric pressure. The vuv system uses two magnesium fluoride lenses and either a Hamamatsu R2083Q (fused silica window) or a Hamamatsu R1220 (magnesium fluoride window) photomultiplier tube, all maintained under the scattering chamber vacuum ( $10^{-4}$  Torr of argon). In either system,

spectral filters can be inserted between the lenses where the fluorescence is roughly collimated. Both systems also contain extensive baffling along the laser-beam paths to reduce scattered light.

Processing of the fluorescence signal from the photomultiplier tube is identical for both the vis-uv and vuv systems. The timing of the laser and atomic pulses is controlled to optimize the LIF signal. The signal is processed by a Tektronix 7912AD transient digitizer, providing an effective analog bandwidth up to 500 MHz. The LIF signals are strong enough (often  $10^4$  or more collected fluorescence photons from each laser shot) that the first several nanoseconds of each decay can be discarded, even for lifetimes as short as 2 ns, providing a pure single exponential decay and eliminating the need to deconvolve the laser excitation pulse. Decay curves are averaged and analyzed by computer to provide a lifetime directly from a least-squares single exponential fit. Reported lifetimes are averages from at least ten separately analyzed decay curves, each of which is an average of 640 LIF shots. The dynamic range of the experiment extends from about 2 ns (electronic bandwidth limited) to about  $2 \mu\text{s}$  (limited by systematic effects due to motion of the atoms relative to the detection system).

Selective laser excitation of a single upper level eliminates repopulation of that level through radiative cascade. However, relatively high-lying levels populated by transitions out of the laser-excited level can sometimes radiate in the spectrally sensitive region of the photomultiplier tube distorting the decay curve. In silicon, this problem occurs when the excited odd-parity upper level (greater than  $50\,000 \text{ cm}^{-1}$ ) has appreciable infrared branches to relatively high-lying even-parity levels which then cascade through infrared or visible transitions to lower odd-parity levels, sometimes with further cascade through visible and ultraviolet transitions to near-ground-state even-parity levels. The relative strength of the cascade channels depends on the initial- and final-state configurations and on the level energy differences. Such cascades are easily blocked by inserting narrow bandpass interference filters between the lenses of the fluorescence collection system. Narrow bandpass filters used in the vuv system have relatively low-peak transmittances (typically 10–15%), but strong fluorescence signals are still routinely detected through the filters. All reported lifetimes were measured using interference filters whenever radiation from cascade through lower levels could conceivably affect the results. In practice, the presence of even small amounts of such cascade radiation is easily detectable as a distortion of the decay curve with substantial apparent lengthening of the lifetime when measurements are made with no spectral filtering of the fluorescence. We limit our study to lifetimes of levels below  $64\,000 \text{ cm}^{-1}$  due to present lack of appropriate spectral filters to block cascade radiation.

Whenever possible, at least two separate excitation wavelengths are used for each upper level, ensuring that the transition is unblended, correctly classified, and correctly identified in the experiment. Several upper levels were cross-checked using both the vis-uv and vuv systems. Agreement between the two systems, coupled with

extensive experience using the vis-uv system, ensures the reliability of the newer vacuum-ultraviolet system

The quoted uncertainty of 5% in the reported lifetimes is a conservative estimate of the combined random and systematic errors. Scatter from separately analyzed decay curves is typically 1% or less for strong signals and 3% or less for the weakest signals. Although strong LIF signals are routine, radiation trapping of transitions in the sputtered silicon atomic beam is not detected—varying the silicon flux by changing the dc or pulsed beam source current has no appreciable effect on the measured lifetimes. Collisional quenching of excited levels is negligible in the atomic beam with low background pressure ( $10^{-4}$  Torr of argon). Possible distortion of the

decay curves due to Zeeman quantum beats is eliminated by making the measurements in a near-zero magnetic field ( $< 20$  mG). Longer lifetimes ( $> 250$  ns) can be measured in a strong magnetic field of 30 G to prevent this distortion, but all silicon lifetimes reported in this paper are under 100 ns. Possible nonlinearities in the fluorescence detection system contribute no more than 2% to the total uncertainty, as demonstrated varying the size of the detected LIF signals. The absolute time base calibration for the 7912AD transient digitizer is provided by a temperature-stabilized oscillator traceable to National Institute of Standards and Technology standards. Measurement of well-established lifetimes in helium provides convincing evidence of the accuracy of the experiment [25].

TABLE I. Measure lifetimes of odd-parity upper levels in neutral silicon.

Configuration and level <sup>a</sup>	Energy (cm <sup>-1</sup> ) <sup>a</sup>	Laser wavelengths (nm) <sup>a</sup>	This experiment	Lifetime (ns)				
				Smith <i>et al.</i> Ref. [5] derived from emission and absorption spectra <sup>b</sup>	Bashkin <i>et al.</i> Ref. [10] beam foil spectroscopy	Becker <i>et al.</i> Ref. [29] laser-induced fluorescence	Savage and Lawrence Ref. [11] phase shift	Marek and Richter Ref. [12] phase shift
4s <sup>3</sup> P <sub>0</sub>	39 683.16	252.411	4.5±0.2	6.3±0.6				5.53±0.44
4s <sup>3</sup> P <sub>1</sub>	39 760.29	251.432 252.851 410.294	4.5±0.2	5.8±0.8				5.39±0.43
4s <sup>3</sup> P <sub>2</sub>	39 955.05	250.690 251.611	4.5±0.2	6.3±0.6	5.9±0.7	4.4±0.4	6.1±0.8	5.95±0.48
4s <sup>1</sup> P <sub>1</sub>	40 991.88	288.158 390.552	4.3±0.2	3.8±0.6	4.1±0.2	4.1±0.4		
3p <sup>3</sup> D <sub>1</sub>	45 276.19	220.798 221.175	22.0±1.1	28±5			18±3	
3p <sup>3</sup> D <sub>2</sub>	45 293.63	221.089 221.806	22.0±1.1	37±9				
3p <sup>3</sup> D <sub>3</sub>	45 321.85	221.667	22.0±1.1	31±5	20.4±1.0			
3d <sup>1</sup> D <sub>2</sub>	47 351.55	243.515	22.5±1.1	17±5	21.3±1.5			
3d <sup>3</sup> P <sub>2</sub>	50 499.84	198.323 198.899	11.4±0.6	15±2				
3d <sup>3</sup> P <sub>1</sub>	50 566.40	197.760 198.636	11.7±0.6	15±2				
3d <sup>3</sup> P <sub>0</sub>	50 602.44	197.921	11.5±0.6	17±2				
3d <sup>1</sup> F <sub>3</sub>	53 362.24	188.185 212.412	3.3±0.2	3.0±0.6	3.0±0.4			
3d <sup>1</sup> P <sub>1</sub>	53 387.33	187.581 212.299 263.128	8.5±0.4	8.6±2.0	8.2±0.1	8.1±0.5		
3d <sup>3</sup> D <sub>1</sub>	54 185.26	184.552 184.815	4.2±0.2	3.8±0.6				
3d <sup>3</sup> D <sub>2</sub>	54 205.09	184.747 185.247	4.0±0.2	4.1±1.4				
3d <sup>3</sup> D <sub>3</sub>	54 257.58	185.067 208.446	4.1±0.2	4.4±2.7				
5s <sup>3</sup> P <sub>0</sub>	54 245.02	184.611	13.8±0.7					
5s <sup>3</sup> P <sub>1</sub>	54 313.82	184.377 184.875	12.6±0.6	8.8±4.0				
5s <sup>3</sup> P <sub>2</sub>	54 528.22	183.651 184.145	13.4±0.7	16±4				
5s <sup>1</sup> P <sub>1</sub>	54 871.03	182.246 205.813 253.238	8.8±0.4	8.9±3.0				

TABLE I. (Continued).

Configuration and level <sup>a</sup>	Energy (cm <sup>-1</sup> ) <sup>a</sup>	Laser wavelengths (nm) <sup>a</sup>	Lifetime (ns)					
			This experiment	Smith <i>et al.</i> Ref. [5] derived from emission and absorption spectra <sup>b</sup>	Bashkin <i>et al.</i> Ref. [10] beam foil spectroscopy	Becker <i>et al.</i> Ref. [29] laser-induced fluorescence	Savage and Lawrence Ref. [11] phase shift	Marek and Richter Ref. [12] phase shift
4d <sup>1</sup> D <sub>2</sub>	56 503.35	177.682	44.5±2.2	69±20				
		199.185						
4d <sup>3</sup> P <sub>2</sub>	56 690.90	176.635	37.2±1.9	35±9				
		177.092						
4d <sup>3</sup> P <sub>1</sub>	56 700.25	176.606	32.4±1.6	37±10				
		177.063						
4d <sup>3</sup> P <sub>0</sub>	56 733.38	176.503	31.9±1.6	58±11				
4d <sup>1</sup> P <sub>1</sub>	58 801.53	170.064	10.8±0.5	2.5±0.6				
		230.306						
4d <sup>1</sup> F <sub>3</sub>	58 893.40	170.444	6.2±0.3	13±4				
		190.134						
4d <sup>3</sup> D <sub>2</sub>	59 032.19	169.621	4.8±0.3	6.3±2.9				
		170.042						
4d <sup>3</sup> D <sub>1</sub>	59 056.51	169.329	5.7±0.3	9±4				
		169.551						
4d <sup>3</sup> D <sub>3</sub>	59 118.03	169.794	4.8±0.3	6.3±1.4				
		189.325						
6s <sub>1/2</sub> ( $\frac{1}{2}, \frac{1}{2}$ ) <sub>0</sub>	59 221.11	169.079	32.7±1.6	28±6				
6s <sub>1/2</sub> ( $\frac{1}{2}, \frac{1}{2}$ ) <sub>1</sub>	59 273.58	168.929	24.7±1.2	23±6				
		169.347						
6s <sub>1/2</sub> ( $\frac{3}{2}, \frac{1}{2}$ ) <sub>2</sub>	59 506.36	168.267	34.6±1.7	31±5				
		168.682						
6s <sub>1/2</sub> ( $\frac{3}{2}, \frac{1}{2}$ ) <sub>1</sub>	59 636.67	167.682	20.0±1.0	1.1±0.3				
		187.484						
3pnd a <sup>3</sup> P <sub>2</sub>	59 917.34	167.112	11.6±0.6	13±2				
		167.521						
3pnd a <sup>3</sup> P <sub>1</sub>	60 010.46	166.852	11.2±0.6	12±2				
		167.260						
3pnd a <sup>3</sup> P <sub>0</sub>	60 042.50	166.763	11.4±0.6					
5d <sup>1</sup> P <sub>1</sub>	61 305.67	163.117	13.4±0.7					
		163.322						
5d <sup>1</sup> F <sub>3</sub>	61 423.23	163.398	10.2±0.5					
		181.408						
5d <sup>3</sup> D <sub>2</sub>	61 447.86	162.944	8.1±0.4	10 <sup>+10</sup> <sub>-5</sub>				
		163.333						
5d <sup>3</sup> D <sub>1</sub>	61 511.77	162.571	16.1±0.8					
		162.775						
5d <sup>3</sup> D <sub>3</sub>	61 574.81	162.995	8.5±0.4	3.6±2.0				
		180.910						
7s <sub>1/2</sub> ( $\frac{1}{2}, \frac{1}{2}$ ) <sub>1</sub>	61 595.43	162.553	23.6±1.2					
		180.843						
7s <sub>1/2</sub> ( $\frac{3}{2}, \frac{1}{2}$ ) <sub>1</sub>	61 881.60	161.801	45.9±2.3					
		179.912						
5d <sup>3</sup> P <sub>2</sub>	61 841.94	162.288	11.1±0.6					
5d <sup>3</sup> P <sub>1</sub>	61 936.13	161.658	11.7±0.6					
		162.040						
5d <sup>3</sup> P <sub>0</sub>	61 960.26	161.595	12.1±0.6					
6d <sup>1</sup> F <sub>3</sub>	62 802.86	159.796	19.2±1.0					
		176.979						

<sup>a</sup> Configurations and level energies are from Martin and Zalubas (Ref. [26]). Wavelengths above 200 nm are air values; wavelengths below 200 nm are vacuum values.

<sup>b</sup> Normalized to the lifetimes reported in Bashkin *et al.* (Ref. [10]).

## EXPERIMENTAL RESULTS

Table I lists the measured lifetimes of 47 odd-parity upper levels in silicon with level energies ranging from 39 000 to 63 000  $\text{cm}^{-1}$  above the ground level, along with previously reported measurements. The laser wavelengths used to excite the upper levels range from 160 to 410 nm, and many of the upper levels are accessible only through vuv excitation. The level energies and configurations are from Ref. [26]. For convenience, six lifetimes previously reported by us in a preliminary Letter are included [27]. Three of these lifetimes, for the  $4d^3D^o$  term, have been slightly shortened compared to our previous report after an electronic bandwidth limitation was discovered in the Hamamatsu R2083Q photomultiplier tube originally used to detect the fluorescence. Single-photon spikes from the R2083Q have a short risetime and falltime ( $< 1$  ns), but a longer low-amplitude tail in the impulse response lengthens the apparent lifetimes of short-lived levels. Subsequently, all short ( $< 8$  ns) lifetimes were measured with at least one of the higher bandwidth photomultiplier tubes—either an RCA 1P28A (visible-uv sensitivity) or a Hamamatsu R1220 (visible-uv-vuv sensitivity)—demonstrated to have sufficient bandwidth to accurately reproduce lifetimes shorter than 3 ns.

Table II and Fig. 3 further compare our results to the other existing lifetime data for silicon. Previously reported lifetimes for some levels vary significantly from our results. However, the average ratios of the results reported here to the previous data generally show good agreement (except for comparison with the results of Marek and Richter [12]) with no obvious systematic errors present. The results of Marek and Richter are based on electron excitation phase-shift measurements which were significantly affected by cascade repopulations. Lifetimes from Smith *et al.* [5] were obtained by normalizing an extensive set of relative transition probabilities (branching ratios) from emission and absorption spectra with the

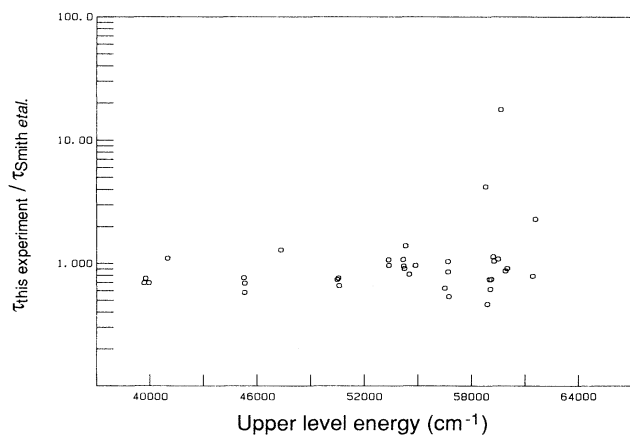


FIG. 3. Comparison of 36 level lifetimes in silicon measured in this experiment with lifetimes determined by Smith *et al.* (Ref. [5]).

radiative lifetimes from Bashkin *et al.* [10]. The overall agreement between our data and those of Smith *et al.* is good, as expected since the level lifetimes chosen for normalization are in good overall agreement with our data. It is encouraging that, except for comparison with Marek and Richter, the overall agreement between our lifetimes and those measured by three different techniques is well within the 5% overall uncertainty assigned to our data. Although the overall agreement between our lifetimes and those previously reported is good, there is substantial scatter in the ratios of individual lifetimes. The only other reported lifetime measurements in silicon were made on six high-lying even parity levels not studied in this experiment [28].

Table III lists absolute transition probabilities ( $A$

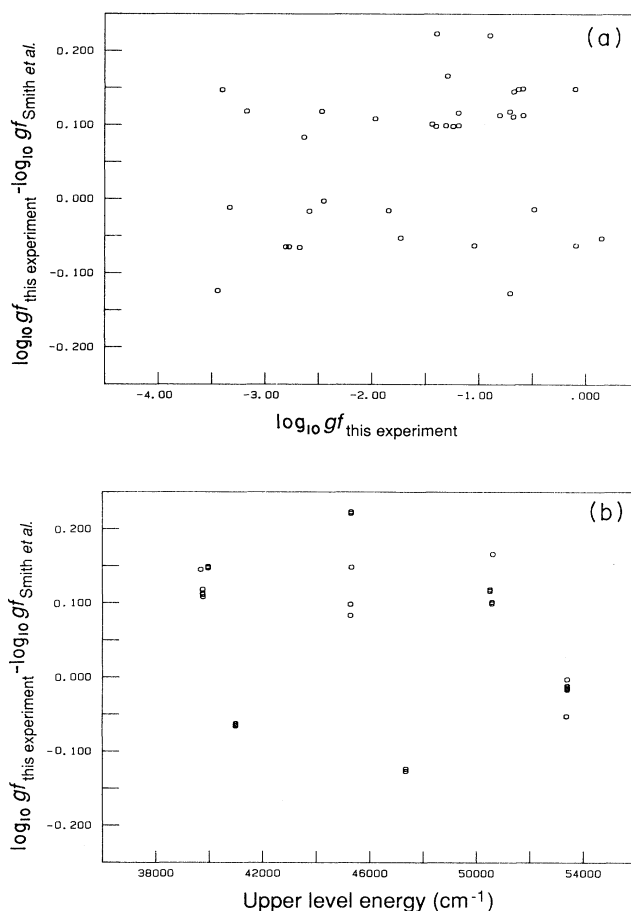


FIG. 4. Comparison of 36 absolute absorption oscillator strengths (as  $\log_{10}gf$  values), deduced from radiative lifetimes measured in this experiment and branching fractions or ratios determined by Smith *et al.* (Ref. [5]), with oscillator strengths measured in emission and absorption by Smith *et al.* (a) Difference of  $\log_{10}gf$  values from this experiment and from Smith *et al.* as a function of  $\log_{10}gf$ . (b) Difference of  $\log_{10}gf$  values as a function of upper-level energy. Several data points are nearly coincident and are not resolved on the scale of this figure.

TABLE II. Comparison of the lifetimes from this experiment to previously reported silicon lifetimes.

	Smith <i>et al.</i> Ref. [5]. derived from emission and absorption spectra <sup>a</sup>	Bashkin <i>et al.</i> Ref. [10] beam foil spectroscopy	Becker <i>et al.</i> Ref. [29] LIF	Savage and Lawrence Ref. [11] phase shift	Marek and Richter Ref. [12] phase shift
$\frac{\tau_{\text{this experiment}}}{\tau_{\text{previous experiment}}}$	1.02±0.66	1.01±0.13	1.04±0.02	0.98±0.34	0.80±0.04
Number of levels compared	35 <sup>b</sup>	6	3	2	3

<sup>a</sup> Normalized to the lifetimes reported in Bashkin *et al.* (Ref. [10]).

<sup>b</sup> The 59 636.67-cm<sup>-1</sup> level is not included in this comparison—the ratio for this level is  $\tau_{\text{this experiment}}/\tau_{\text{Smith et al.}} = 18.2$ .

values) and absorption oscillator strengths (as  $\log_{10}gf$  values) for 36 visible, uv, and vuv transitions out of 13 of the lowest-lying odd-parity levels in silicon. The transition probabilities are derived by combining our measured lifetimes with the branching fraction or branching ratio

data of Smith *et al.* [5]. Smith *et al.* directly report their branching ratios to an absolute precision of  $\pm 0.001$ , but greater precision for small branches ( $< 0.050$ ) can be achieved by deducing the branching ratios from their relative reported  $\log_{10}gf$  values for all transitions to a given

TABLE III. Absolute transition probabilities ( $A$  values) and absorption oscillator strengths (as  $\log_{10}gf$ ) in Si I.

Upper level	Lower level (configuration $3p^2$ )	Transition wavelength (nm) <sup>a</sup>	$A$ ( $10^6 \text{ sec}^{-1}$ )	$\log_{10}gf$ (this experiment)	$\log_{10}gf$ (Smith <i>et al.</i> Ref. [5])
4s $^3P_0^\circ$	$^3P_1$	252.411	222±11	-0.673±0.021	-0.82±0.07
4s $^3P_1^\circ$	$^3P_0$	251.432	74.0±3.8	-0.677±0.022	-0.79±0.07
	$^3P_1$	251.920	54.9±2.9	-0.805±0.022	-0.92±0.07
	$^3P_2$	252.851	90.4±4.6	-0.585±0.022	-0.70±0.07
	$^1D_2$	298.765	2.67±0.25	-1.970±0.039	-2.08±0.14
	$^1S_0$	410.294	<0.44±0.14	<-2.47±0.12	<-2.59±0.13
4s $^3P_2^\circ$	$^3P_1$	250.690	54.7±2.8	-0.589±0.022	-0.74±0.07
	$^3P_2$	251.611	168±8	-0.099±0.022	-0.25±0.07
	$^1D_2$	297.036	0.0600±0.0084	-3.401±0.057	-3.55±0.07
4s $^1P_1^\circ$	$^3P_0$	243.877	0.791±0.061	-2.674±0.032	-2.61±0.07
	$^3P_1$	244.336	0.628±0.057	-2.773±0.037	-2.71±0.07
	$^3P_2$	245.212	0.581±0.059	-2.803±0.042	-2.74±0.07
	$^1D_2$	288.158	217±11	-0.091±0.021	-0.03±0.07
	$^1S_0$	390.552	13.3±0.7	-1.041±0.023	-0.98±0.07
3p $^3D_1^\circ$	$^3P_0$	220.798	26.2±1.4	-1.240±0.022	-1.34±0.07
	$^3P_1$	221.174	18.1±1.0	-1.400±0.023	-1.50±0.07
	$^3P_2$	221.892	1.05±0.15	-2.635±0.057	-2.72±0.08
3p $^3D_2^\circ$	$^3P_1$	221.089	34.5±1.7	-0.897±0.021	-1.12±0.10
	$^3P_2$	221.806	10.9±0.6	-1.395±0.022	-1.62±0.10
3p $^3D_3^\circ$	$^3P_2$	221.667	45.4±2.3	-0.630±0.021	-0.78±0.08
3d $^1D_2^\circ$	$^3P_2$	212.119	0.107±0.015	-3.442±0.057	-3.32±0.17
	$^1D_2$	243.515	44.3±2.2	-0.705±0.021	-0.58±0.11
3d $^3P_2^\circ$	$^3P_1$	198.323	21.8±1.1	-1.192±0.021	-1.31±0.12
	$^3P_2$	198.899	65.7±3.3	-0.710±0.021	-0.83±0.12
	$^1D_2$	226.169	<0.175±0.045	<-3.17±0.10	<-3.29±0.11
3d $^3P_1^\circ$	$^3P_0$	197.760	27.9±1.4	-1.309±0.021	-1.41±0.12
	$^3P_1$	198.062	20.7±1.1	-1.437±0.022	-1.54±0.12
	$^3P_2$	198.636	36.5±1.8	-1.189±0.021	-1.29±0.12
3d $^3P_0^\circ$	$^3P_1$	197.921	87.0±4.3	-1.292±0.021	-1.46±0.07
3d $^1F_3^\circ$	$^3P_2$	188.185	5.00±0.60	-1.731±0.050	-1.68±0.09
	$^1D_2$	212.412	298±15	+0.149±0.021	+0.20±0.08
3d $^1P_1^\circ$	$^3P_0$	187.310	1.65±0.18	-2.585±0.046	-2.57±0.11
	$^3P_1$	187.582	2.24±0.26	-2.451±0.048	-2.45±0.11
	$^3P_2$	188.097	0.294±0.029	-3.330±0.039	-3.32±0.11
	$^1D_2$	212.299	7.1±1.3	-1.84±0.07	-1.83±0.12
	$^1S_0$	263.128	106±5	-0.482±0.022	-0.47±0.11

<sup>a</sup> Air values are listed for wavelengths above 200 nm, vacuum values for wavelengths below 200 nm.

upper level. The uncertainty in our reported values results from the combination in quadrature of the uncertainty in the lifetimes with the branching fraction/ratio uncertainty reported by Smith *et al.* Most of the total uncertainties are between 5–10%. Transition probabilities are not calculated for a few very weak lines (branching fractions or ratios given by Smith *et al.* as “<0.000”). Figure 4 graphically compares the  $\log_{10}gf$  values from this experiment with those obtained by Smith *et al.* from emission and absorption measurements. The overall agreement is good—the mean of  $(\log_{10}gf_{\text{this experiment}} - \log_{10}gf_{\text{Smith et al.}})$  is 0.060 with a standard deviation of 0.096. The difference of the  $\log_{10}gf$  values does not appreciably depend on the magnitude of  $gf$  or the energy of the upper level.

The extensive branching ratio data reported by Smith *et al.* would seem to be ideally suited for combination with our radiative lifetimes to generate a comprehensive set of absolute transition probabilities. However, Smith *et al.* limited their measurements to the spectral range 160–410 nm and did not report any data on infrared transitions. Instead, they relied on semiempirical calculations to estimate the intensity of the infrared decay channels. It is difficult to accurately calculate such strong infrared transitions. We found that virtually every level above the  $3d^1P_1^o$  level at  $53\,387\text{ cm}^{-1}$  exhibited substantial lengthening of the observed lifetime when the LIF was detected without spectral filtering, indicating significant infrared decay channels to nearby lower-lying levels which then radiate in the visible, uv, or vuv. (All reported lifetimes are based on data collected with spectral filters that blocked all such cascade radiation.) While Smith *et al.* have determined an important set of branching ratios for transitions in the 160–410-nm range, the branching fractions (including all possible transitions out of the level) needed for determination of accurate absolute transition probabilities are more uncertain for levels above the  $3d^1P_1^o$  level at  $53\,387\text{ cm}^{-1}$ . Transition probabilities for infrared lines from the 13 lowest-lying odd

parity levels are suppressed by either Russell-Saunders (*LS*) selection rules or by the extremely low frequencies of the infrared transitions. The dominant transitions from all of these 13 levels have branching fractions or ratios (as measured by Smith *et al.*) in very good agreement with predicted pure Russell-Saunders branching fractions, as expected for a light element such as silicon. In addition, the apparent lifetimes for the 13 lowest levels are not detectably altered when observed with and without spectral filtering of the LIF, supporting the assumption that the infrared transitions out of these levels are insignificant. (Significant infrared transitions out of these levels would lead to cascade radiation in the spectral bandpass of the unfiltered PMT. Even a small amount of such cascade radiation tends to appreciably lengthen the apparent lifetime.) We therefore conservatively choose to report absolute transition probabilities only through the  $3d^1P_1^o$  level. A more accurate determination of the strengths of infrared transitions out of the higher-lying levels ( $> 53\,400\text{ cm}^{-1}$ ) is needed before the lifetimes reported here can be confidently combined with the branching ratios of Smith *et al.* to generate absolute transition probabilities for those higher levels.

The data reported in this article provide a significantly more accurate and extensive base than previously available for either normalizing relative transition probabilities or determining absolute transition probabilities in combination with branching fraction measurements, and demonstrates the potential of our vuv system for measuring extensive sets of lifetimes for almost any element.

#### ACKNOWLEDGMENTS

This research was supported by NASA Grant No. NAG 5-1048 and NSF Grant No. AST-88-21051. We acknowledge the contributions of E. C. Benck in the development of the vacuum-ultraviolet laser system.

\*Present address: National Institute of Standards and Technology, Gaithersburg, MD 20899.

- [1] E. Anders and N. Grevesse, *Geochim. Cosmochim. Acta* **53**, 197 (1989).
- [2] B. Gustafsson, *Phys. Scr.* **T34**, 14 (1991).
- [3] N. Grevesse, *Phys. Scr.* **T8**, 49 (1984).
- [4] T. Garz, *Astron. Astrophys.* **26**, 471 (1973).
- [5] P. L. Smith, M. C. E. Huber, G. P. Tozzi, H. E. Griessinger, B. L. Cardon, and G. G. Lombardi, *Astrophys. J.* **322**, 573 (1987).
- [6] J. E. Lawler, in *Lasers, Spectroscopy, and New Ideas: A Tribute to Arthur L. Schawlow*, edited by W. M. Yen and M. D. Levenson (Springer, Berlin, 1988), p. 125.
- [7] W. Whaling, P. Hannaford, R. M. Lowe, E. Biemont, and N. Grevesse, *Astron. Astrophys.* **153**, 109 (1985).
- [8] W. Whaling and J. W. Brault, *Phys. Scr.* **38**, 707 (1988).
- [9] T. R. O'Brian, M. E. Wickliffe, J. E. Lawler, W. Whaling, and J. W. Brault, *J. Opt. Soc. Am. B* **8**, 1185 (1991).
- [10] S. Bashkin, G. Astner, S. Mannervik, P. S. Ramanujam, M. Scofield, S. Hultdt, and I. Martinson, *Phys. Scr.* **21**, 820 (1980).
- [11] B. D. Savage and G. M. Lawrence, *Astrophys. J.* **146**, 940 (1966).
- [12] J. Marek and J. Richter, *Astron. Astrophys.* **26**, 155 (1973).
- [13] L. J. Curtis, in *Beam Foil Spectroscopy*, edited by S. Bashkin (Springer, Berlin, 1976), p. 63.
- [14] J. Carlsson, L. Sturesson, and S. Svanberg, *Z. Phys. D* **11**, 287 (1989).
- [15] D. W. Duquette, S. Salih, and J. E. Lawler, *Phys. Lett.* **83A**, 214 (1981).
- [16] S. Salih and J. E. Lawler, *Phys. Rev. A* **28**, 3653 (1983).
- [17] D. W. Duquette and J. E. Lawler, *Phys. Rev. A* **26**, 330 (1982).
- [18] C. C. Lim, *Rev. Sci. Instrum.* **57**, 108 (1986).
- [19] T. Namioka, H. Noda, and M. Seya, *Sci. Light* **22**, 77 (1973).
- [20] W. K. Bischel, D. J. Bamford, and M. J. Dyer, *Proc.*

- SPIE—Int. Soc. Opt. Eng. **912**, 191 (1988).
- [21] H. Wallmeier and H. Zacharias, *Appl. Phys. B* **45**, 263 (1988).
- [22] R. Mahon and F. S. Tomkins, *IEEE J. Quantum Electron.* **18**, 913 (1982).
- [23] R. Hilbig and R. Wallenstein, *IEEE J. Quantum Electron.* **19**, 1759 (1983).
- [24] P. R. Herman and B. P. Stoicheff, *Opt. Lett.* **10**, 502 (1985).
- [25] S. Salih, J. E. Lawler, and W. Whaling, *Phys. Rev. A* **31**, 744 (1985).
- [26] W. C. Martin and R. Zalubas, *J. Phys. Chem. Ref. Data* **12**, 323 (1983).
- [27] T. R. O'Brian and J. E. Lawler, *Phys. Lett. A* **152**, 407 (1991).
- [28] H. Bergstrom, G. W. Farris, H. Hallstadius, H. Lundberg, and A. Persson, *Z. Phys. D* **13**, 29 (1989).
- [29] U. Becker, H. Kerkhoff, M. Kwiatkowski, M. Schmidt, U. Teppner, and P. Zimmermann, *Phys. Lett.* **76A**, 125 (1980).